Colloid Polym Sci 279:829–835 (2001)

ORIGINAL CONTRIBUTION

B. Guilleaume
M. Ballauff
G. Goerigk
M. Wittemann
M. Rehahn

Correlation of counterions with rodlike macroions as assessed by anomalous small-angle X-ray scattering

Received: 11 December 2000
Accepted: 22 February 2001

B. Guilleaume · M. Ballauff (✉)
Polymer-Institut, Universität Karlsruhe
Kaiserstrasse 12, 76128 Karlsruhe
Germany

G. Goerigk
Institut für Festkörperforschung
Forschungszentrum Jülich, Postfach 1913
52425 Jülich, Germany

M. Wittemann · M. Rehahn
Institut für Makromolekulare Chemie
Petersenstrasse 22, 64287 Darmstadt
Germany

Abstract We consider the analysis of a rodlike synthetic polyelectrolyte in solution by anomalous small-angle X-ray scattering (ASAXS) in order to elucidate the correlation of the counterions with the highly charged macroion. ASAXS can be applied to these systems because the absorption edge of typical counterions, for example, bromine or iodine ions can be attained by synchrotron radiation. Model calculations using the Poisson–Boltzmann cell model show that ASAXS furnishes two terms caused by the anomalous dispersion of the counterions. The leading terms is a cross-term between the ordinary scattering amplitude of the polyelectrolyte and the real part of the scattering length f' of the counterions. A second term refers solely to the anomalous contribution of the counterions, i.e., to f' and f'' (f'': imaginary part of scattering length). Preliminary data obtained from rodlike synthetic macroions having iodine counterions corroborate the theoretical deductions. They demonstrate that ASAXS is capable of furnishing information that is not available by the ordinary SAXS experiment.

Key words Anomalous small-angle X-ray scattering · Small-angle X-ray scattering · Polyelectrolytes · Poisson–Boltzmann cell model · Anomalous dispersion

Introduction

Polyelectrolytes consist of long polymeric structures to which ionogenic groups are attached. When immersed in polar solvents polyelectrolytes dissociate into macroions and their respective counterions [1–4]. The distribution of the counterions around the highly charged macroions is among the oldest problems in this field. Owing to the high electric field of the macroion a part of the counterions will be highly correlated with the macroion, i.e., a fraction of the counterions will be located in the immediate neighborhood of the macroion [5, 6, 7, 8]. If the macroion assumes a rodlike shape, the radial distribution function of the counterions can be calculated by means of the Poisson–Boltzmann (PB) cell model in an analytical fashion [5, 6, 7]. Since polyelectrolytes have great importance in technical applications and biological systems, a quantitative comparison of measured and calculated distribution functions of counterions around a macroion is of general interest [2, 3].

Scattering methods are well suited to investigate the correlation of the counterions with a highly charged macroion in a quantitative fashion. Up to now, small-angle neutron scattering (SANS) has been repeatedly used to study the counterion cloud around rodlike polyelectrolytes, such as DNA dissolved in water (see Refs. [9–12] and further citations given there). The partial contributions of the macroion and of the counterion to the measured SANS intensity, $I(q)$, where $q = (4\pi/\lambda)\sin(\theta/2)$, λ is the wavelength of the radiation used and θ is the scattering angle, can be determined by adjusting the contrast by appropriate mixtures of H_2O and D_2O [13]. SANS, however, requires deuterated counterions to achieve sufficient contrast.

Small-angle X-ray scattering (SAXS) may be used to circumvent this problem. Counterions with sufficiently high atomic number, such as Cs^+ or I^-, exhibit sufficient X-ray contrast. If the macroion itself exhibits only a low excess electron density, the measured SAXS intensity originates mainly from the counterions. In this case SAXS is suitable to assess the distribution of counterions around a rodlike macroion. SAXS, however, allows only the measurement of a combination of all partial contributions to the scattering intensity [14, 15]. Recently, we could show that SAXS allows the study of synthetic rodlike polyelectrolytes if the contrast of the counterions is strong enough [16]. The contrast of the macroion could not be determined in an independent manner, however, but had to be treated as a fit parameter.

In principle, anomalous SAXS (ASAXS) is suitable to overcome this problem [17, 18]: Here counterions can be used with an absorption edge that lies in the energy range of ASAXS beamlines [19]. By appropriate change of the energy of the incident X-rays the resonant contribution of the counterions could be assessed separately from the nonresonant contribution of the macroion. If the contrast variation thus achieved is high enough, an analysis of the distribution of counterions should become possible.

Up to now ASAXS has mostly been used for solid systems, for example, catalysts [20], glasses, alloys and semiconductors [21, 22], or solid ionomers [23, 24]. The number of studies devoted to dissolved polyelectrolytes, however, is scarce [17, 18, 25, 26]. Here we present a study of rodlike polyelectrolytes by ASAXS in aqueous solution. The chemical structure of the repeating unit is shown in Scheme 1. The macroion consists of a poly(*p*-phenylene) backbone. It is stiff enough to be treated as rodlike [16]. Each repeating unit bears four iodine counterions.

The aim of this investigation is twofold. We wish to present a comprehensive theoretical study of the scattering function of rodlike polyelectrolytes when counterions with resonant contributions are present and we present preliminary data on ASAXS data measured on a synthetic stiff-chain polyelectrolyte. The general goal is to obtain the distribution of counterions by ASAXS.

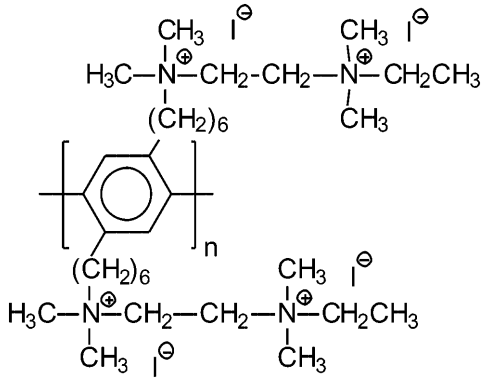

Scheme 1

All measurements were made by use of the JUSIFA beamline at HASYLAB, DESY, Hamburg. The K edge of the iodine counterions is located at 33.170 keV. The choice of iodine counterions derives from the fact, however, that a comprehensive investigation of the same polyelectrolyte by conventional SAXS [16] has been done already. The results obtained in the study by SAXS can directly be used to predict the ASAXS intensities. In this manner a feasibility study of ASAXS experiments as applied to linear polyelectrolytes can be done. Moreover, it will be shown that ASAXS allows the assessment of the contrast of the macroion and thus furnishes information not available by the conventional SAXS experiment.

Theory

We consider a dilute solution of monodisperse rodlike polyelectrolyte molecules dispersed in water. The macroions consist of elements with neglectable anomalous scattering in the energy range given in the experiment. Only the counterions are assumed to give an anomalous contribution to the measured intensity. Since the electron density of the counterions becomes a complex function [17], the calculation of the intensity requires special consideration. In the following the latter contribution is calculated explicitly and studied by use of model calculations.

The absolute scattering intensities, $I(q)$, following from a small-angle scattering experiment is given by [13]

$$I(q) = \frac{N}{V} I_0(q) S(q) \quad , \tag{1}$$

where N/V is the number of dissolved polyelectrolyte molecules per unit volume. $S(q)$ is the effective structure factor, which takes into account the effect of intermolecular interference; for the low concentrations under consideration here its influence is restricted to the region of small scattering angles [16] and will not be considered further here. The total scattering intensity of a system of noninteracting rods follows therefore from Eq. (1) with $S(q) = 1$.

The scattering intensity, $I_0(q)$, of a single rodlike polyelectrolyte molecule follows as an average over all orientations with regard to the scattering vector, $\bar{q}$. It can be formulated as [17, 18]

$$I_0(q) = \int_0^1 F(q,\alpha) F^*(q,\alpha) \mathrm{d}\alpha = \langle F(q,\alpha) F^*(q,\alpha) \rangle_\Omega \quad , \tag{2}$$

where α is the cosine of the angle between $\bar{q}$ and the long axis of the molecule. The scattering amplitude, $F(q,\alpha)$, of the rod with orientation α follows as [27]

$$F(q,\alpha) = L\frac{\sin(q\alpha L/2)}{q\alpha L/2}\int_0^\infty \Delta\rho(r_c)J_0[qr_c(1-\alpha^2)^{1/2}]2\pi r_c\,dr_c$$
$$= L\frac{\sin(q\alpha L/2)}{q\alpha L/2}F_{cr}[\Delta\rho(r_c),q,\alpha]\ . \quad (3)$$

Here $\Delta\rho(r_c)$ is the radial excess electron density of the dissolved polyelectrolyte versus the surrounding medium. It includes the real excess electron density of the macroion itself and the complex electron density of its counterions. $F(q,\alpha)$ can thus be related to the Hankel transform, $F_{cr}[\Delta\rho(r_c),q,\alpha]$, of the radial excess electron density, $\Delta\rho(r_c)$, of a single polyelectrolyte molecule. From its derivation it is evident that Eq. (3) holds true for complex excess scattering length density as well. It must be noted, however, that $F(q,\alpha)$ becomes a complex quantity if $\Delta\rho(r_c)$ is complex.

For $q > 1/L$, Eqs. (2) and (3) can be simplified considerably. In this case the main part of scattering of a rodlike object results if $\bar{q}$ is perpendicular to the long axis of the rod, i.e., when $\alpha \approx 0$. Thus,

$$I_0(q) \to L\frac{\pi}{q}F_{cr}[\Delta\rho(r_c),q,\alpha=0]F^*_{cr}[\Delta\rho(r_c),q,\alpha=0] \quad (4)$$

if q is sufficiently high. The measured intensity multiplied by q therefore gives the square of the Hankel transform of the cross-sectional excess electron density distribution to a good approximation. It is therefore evident that a small-angle scattering experiment furnishes direct information about the radial distribution of the counterions, which is difficult to obtain by any other method.

It has been suggested to expand $F_{cr}[\Delta\rho(r_c),q,\alpha=0]$ in Eq. (4) into a series in powers of q^2 [17]. The coefficient of this expansion is the radius of gyration of the scattering length distribution perpendicular to the long axis of the rod [13, 17]. Model calculations using the PB cell model show, however, that the minimum q value at which the first meaningful experimental data points can be taken is not small enough to restrict the expansion to terms up to q^2. Hence, the results of the full calculation must be compared to experimental data.

As in Ref. [16] the macroion can be described in terms of a constant real excess electron density, $\Delta\rho_{rod}$. Let a define the minimum distance of approach between the macroion and the counterions. In the following model calculation within the frame of the PB cell model the counterions are approximated as pointlike. Hence, the parameter a is the radius of the macroion at the same time. Therefore $\Delta\rho(r_c) = \Delta\rho_{rod}$ for $r_c \le a$. For $r_c > a$ the excess electron density is entirely determined by the counterions. The integration in Eq. (3) must be extended over all counterions belonging to one macroion, otherwise the condition of electroneutrality would be violated. Let Δf_{ion} denote the number of excess electrons per counterion. Then $\Delta\rho(r_c) = \Delta f_{ion} n(r_c)$ for radial distances $r_c > a$, where $n(r_c)$ denotes the radial number density of counterions. Hence, the calculation of $I(q)$ requires the determination of Δf_{ion} as well as of the distribution function $n(r_c)$.

Scattering length density of counterions

Near the absorption edge the scattering length of a single counterion becomes an explicit function of the energy, E, of the incident X-rays [28]. It may be expressed through [17, 18, 28]

$$f = f_0 + f'(E) + if''(E)\ . \quad (5)$$

The first term, f_0, is the nonresonant term, which is equal to the atomic number of the element. The second and the third factors are energy-dependent and show a strong variation only in the vicinity of the absorption edge. The imaginary part, f'', is directly related to the absorption cross-section of the X-rays and both f' and f'' are connected to each other by the Kramers–Kronig relation. Both quantities can be calculated by the routine furnished by Cromer and Liberman [29].

For ions immersed in a medium of scattering length density ρ_m the contrast per ion follows as

$$\Delta\rho_{ion} = \frac{f}{V_{ion}} - \rho_m\ , \quad (6)$$

where V_{ion} denotes the volume of a given ion. V_{ion} must be calculated from the density of the polyelectrolyte in solution. Calculated per counterion we have

$$\Delta f_{ion} = f_0 - \rho_m V_{ion} + f' + if'' \quad (7)$$

Here it becomes obvious that the dispersive part of f does not depend on the electron density of the solvent. Thus, ASAXS furnishes information which is directly related to the counterions and not to their contrast towards the surrounding medium.

Calculation of $n(r_c)$

The distribution function $n(r_c)$ may be calculated from the solution of the PB equation within the frame of the cell model. Van der Maarel and coworkers [9, 10, 11, 12] have demonstrated that the PB cell model provides a valid approach for rodlike polyelectrolytes. Within the frame of this model, the polyelectrolyte is characterized by the charge parameter, ξ, which is defined through the ratio of the Bjerrum length, λ_B, to the contour distance per unit charge, b:

$$\xi = \frac{\lambda_B}{b}\ , \quad (8)$$

with λ_B being defined through

$$\lambda_B = \frac{e^2}{4\pi\varepsilon_0\varepsilon k_B T} \quad , \tag{9}$$

where e is unit charge, ε the dielectric constant of the medium and ε_0, k_B and T have their usual meanings. In order to obtain $n(r_c)$ the solution of uniform cylindrical polyelectrolytes of length L is treated as a system of N parallel rods. The cell radius, R_0, follows from the number concentration, N/V, of the rods as $(N/V)\ \pi R_0^2 L = 1$. $n(r_c)$ is given by

$$\frac{n(r_c)}{n(R_0)} = \left(\frac{2|\beta|}{\kappa r_c \cos[\beta \ln(r_c/R_M)]}\right)^2 \quad . \tag{10}$$

From the known parameters ξ, a and R_0 the first integration constant, β, can be obtained through

$$\arctan\left(\frac{\xi-1}{\beta}\right) + \arctan\left(\frac{1}{\beta}\right) - \beta \ln\left(\frac{R_0}{a}\right) = 0 \quad . \tag{11}$$

The second integration constant, R_M, may be regarded as the radial distance in which the counterions are condensed [7]. It follows as

$$R_M = a\ \exp\left[\frac{1}{\beta}\arctan\left(\frac{\xi-1}{\beta}\right)\right] \quad . \tag{12}$$

The screening constant, κ, and the number, $n(R_0)$, of counterions at the cell boundary are related through $\kappa = 8\pi\lambda_B n(R_0) = 4(1+\beta^2)/{R_0}^2$.

Calculation of energy-dependent terms of $I(q)$

With $n(r_c)$ being known, the excess electron density within the cell, i.e., for $a \le r_c \le R_0$ the integration Eq. (3) can be performed. Hence, $\Delta\rho(r_c)$ follows as

$$\begin{aligned} &= \Delta\rho_{rod} \quad 0 \le r_c \le a \\ \Delta\rho(r_c) &= n(r_c)\Delta f_{ion} \quad a < r_c \le R_0 \\ &= 0 \qquad\qquad\quad r_c > R_0 \end{aligned} \tag{13}$$

Hence, $\Delta\rho(r_c)$ may be split into a nonresonant term, $\Delta\rho_0(r_c)$, and the resonant contributions of the counterions

$$\Delta\rho(r_c) = \Delta\rho_0(r_c) + n(r_c)f' + in(r_c)f'' \quad . \tag{14}$$

The scattering amplitude resulting from insertion of Eq. (13) into Eq. (3) may be split into a nonresonant term and two resonant terms depending on the energy of the incident X-rays

$$\begin{aligned} &F(q,\alpha)F^*(q,\alpha) \\ &= \left(L\frac{\sin(q\alpha L/2)}{q\alpha L/2}\right)^2 \Big\{F_{cr}^2[\Delta\rho_0(r_c),q,\alpha] \\ &\quad + 2f' F_{cr}[\Delta\rho_0(r_c),q,\alpha]F_{cr}[n(r_c),q,\alpha] \\ &\quad + \left(f'^2 + f''^2\right)F_{cr}^2[n(r_c),q,\alpha]\Big\} \quad . \end{aligned} \tag{15}$$

Insertion of Eq. (15) into Eq. (2) leads to the measured intensity, which consists of three parts. The first term of Eq. (15) describes the scattering intensity measured at energies far apart from the resonance energy. This term is solely related to the nonresonant contribution, f_0. The second expression in Eq. (15) is the cross-term of the nonresonant amplitude with the term related to f'. The third expression may be regarded as the self-term of the resonant scatterers. Subtracting the nonresonant term from the measured intensity leads, therefore, to two terms related to f' and f''.

Equation (15) is the central result of the present analysis. It demonstrates that ASAXS in the case of polyelectrolytes gives a mixed resonant contribution which is not solely due to the resonant species in the system. Only if the macroion is virtually matched by the surrounding solvent does the cross term vanish and the third term of Eq. (15) governs the measured intensity. This is not the case for most systems of practical importance, however, and usually both terms must be considered.

Model calculation

To elucidate the main points of the preceding theoretical considerations, we discuss the ASAXS intensity obtained from a model calculation. All calculations discussed subsequently are done with the use of Eqs.(2) and (3). The model parameters are chosen to match the experimental system studied experimentally. We assume rodlike macroions of uniform length. Additional model calculations have demonstrated that the influence of polydispersity is rather small unless one confines the analysis to the lowest q values. The length of the macroion was set to 20 nm and the charge parameter (cf. Eq. 8) $\xi = 6.65$. The contact distance, a (cf. Eq. 13), is 0.8 nm and the cell radius, R_0 (see Eq. 13), is 8.43 nm. This corresponds to a weight concentration of the polyelectrolyte of 2 wt%. With these parameters being fixed, the radial distribution of the counterions may be calculated through use of Eqs. (10), (11) and (12).

The contrast parameters are chosen as follows: For I^- we take the value resulting for iodine ions in water, which is $\Delta f_{ion} = 39$e/ion. Here it was assumed that the unhydrated ions are embedded in water of macroscopic density. Hence, the crystallographic radius of 0.22 nm [30] for the iodine was used. For the contrast of the macroion a low value of 2e/nm^3 was assumed. The f' and f'' values for iodine were calculated according to Cromer and Liberman [29]. The data calculated for the respective wavelengths are gathered in Table 1.

The results of calculations for 33.169 keV using the respective data of Table 1 are shown in Fig. 1. It becomes evident that there is an appreciable difference

between the SAXS intensity measured away from the edge (32 keV; solid line) and the one taken in the immediate neighborhood of the edge (33.169 keV; dashed line). Moreover, $I(q)$ measured in the immediate neighborhood of the edge runs virtually parallel to the intensity measured far away from the edge. The same is true for the difference of both terms. If the energy of the incident radiation is changed, i.e., if the parameters f' and f'' are changed accordingly, the scattering curves are shifted nearly parallel to the ordinate. This may be traced back to the strong contrast of the counterions that hence dominate the measured intensity.

The self-term (marked by crosses in Fig. 1) is small but becomes important at higher q values when the nonresonant term has its minimum. For the present set of model parameters it is of opposite sign to the cross-term in Eq. (15). If the contrast of the macroion is low, the cross-term will be small accordingly and the self-term may even become the leading term at the highest q values. It is hence evident that both resonant terms must be taken into account when discussing dissolved polyelectrolytes.

It also shows that ASAXS is sensitive towards the magnitude and the sign of the contrast, $\Delta\rho_{\mathrm{rod}}$, of the macroion: For a high contrast of the macroion the cross-term will govern the resonant contribution to the intensity. In this case Eq. (15) directly demonstrates that the ratio of this contribution measured at two different energies, E_1 and E_2, must be $f'(E_1)/f'(E_2)$.

Table 1 Values of f' and f'' at different energies

Energy/keV	f' (electrons)	f'' (electrons)
32.000	−3.09	0.608
33.030	−4.98	0.57
33.150	−6.81	0.57
33.169	−10.1	3.52

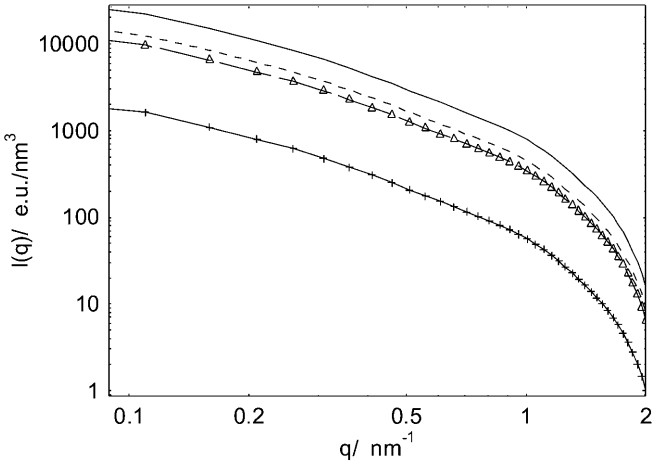

Fig. 1 Model calculation with positive contrast of macroion. Parameters: charge parameter of macroion $\xi = 6.65$; contact distance $a = 0.8$ nm; cell radius $R = 8.43$ nm; the contrast of the iodine ions far from the absorption edge was set to $\Delta f_0 = 39$e/ion. The electron density of the macroion was $\Delta\rho_{\mathrm{rod}} = 2\mathrm{e/nm}^3$. For f' and f'' the data in Table 1 were used. *Solid line*: nonresonant small-angle X-ray scattering (*SAXS*) intensity; *short-dashed line*: intensity calculated for 33.169 keV; *dashed line marked by triangles*: calculated difference between SAXS and anomalous SAXS (*ASAXS*) intensity; *dashed line marked by crosses*: self-term

Experimental

All measurements reported here are made at the JUSIFA beamline, HASYLAB, DESY, Hamburg. The K edge of iodine was determined by measurements of KI salt (theoretical value: 33.169 keV).

Only salt-free solutions of the polyelectrolyte shown in Scheme 1 were investigated. The polyelectrolyte was dissolved in pure water and confined in capillaries of 2-mm diameter. This length of the optical path was not the optimal one but was necessary owing to the limited amount of material. Measurements are made at three different energies, namely 32.000, 33.150 and 33.167 keV. All the data were corrected for absorption, dark current, background scattering and detector sensitivity and were calibrated into absolute units of macroscopic cross-sections. The scattering data discussed here were circularly averaged using the software available at the beamline [19]. To ensure a meaningful comparison with data measured with a different camera, the scattering intensity of water was used to check the calibration of the instrument.

Calibrated scattering curves measured at four different energies are shown in Fig. 2. For comparison an additional scattering curve is shown which represents the scattering of water. Data taken in the immediate vicinity of the edge (33.150 and 33.169 keV) are afflicted by an energy-dependent constant background due to fluorescence. This effect is most clearly visible when taking data in the immediate vicinity of the absorption edge (33.169 keV; crosses in Fig. 2). The magnitude of the fluorescence can be determined from the respective data at high q values without problems. It is subtracted

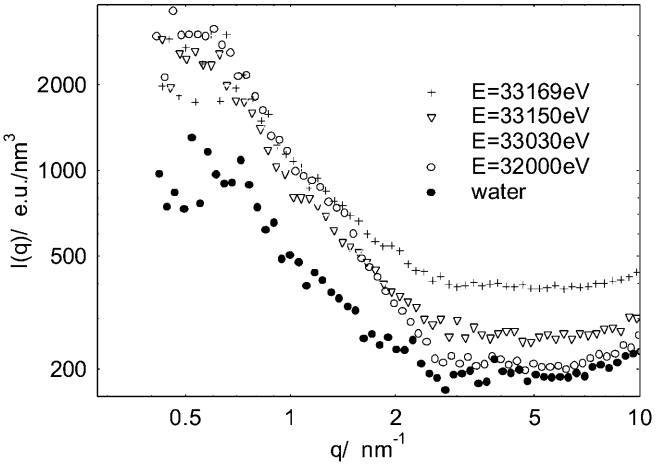

Fig. 2 Absolute scattering intensities of the polyelectrolyte solution measured at different energies of the incident radiation indicated on the graph

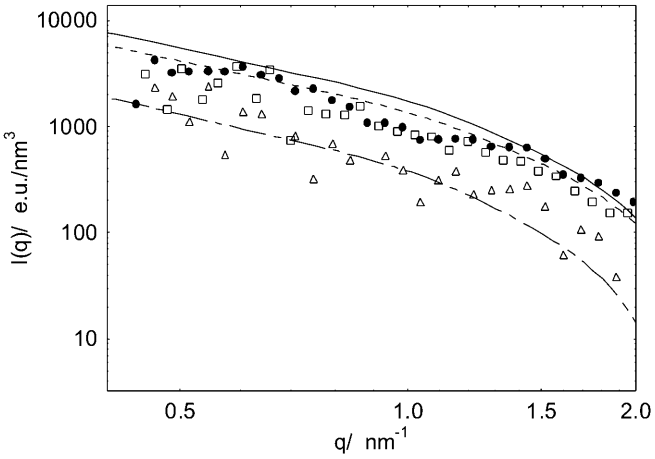

Fig. 3 Comparison of theoretical calculations and experimental data. All experimental intensities were corrected for fluorescence and the background scattering of the solvent water. The *filled circles* mark the experimental intensity measured at 32.000 keV, whereas the *open squares* mark the intensities measured at 33.169 keV. *Open triangles* mark the difference between the two experimental intensities. *Solid line*: ASAXS intensity calculated for 32.000 eV according to Eq. (15); *short-dashed line*: intensity calculated for 33.169 keV; *dashed-dotted line*: calculated difference between the intensities calculated for 32.000 and 33.169 keV. Parameters: charge parameter of macroion $\xi = 6.65$; contact distance $a = 0.8$ nm; cell radius $R = 8.43$ nm; $\Delta\rho_{\mathrm{rod}} = 25\mathrm{e/nm}^3$. The contrast of the iodine ions far from the absorption edge was set to $\Delta f_0 = 39$e/ion. For f' and f'' the data in Table 1 were used

as a constant contribution from the data. After correction for fluorescence the difference of the scattering intensities determined at different energies can be compared to the theoretical predictions.

Results and discussion

The absolute intensities measured at different energies of incident radiation are displayed in Fig. 3. The data were corrected for the background contribution of the solvent water and the contribution of fluorescence.

The subtraction suggested by Eq. (15) can be carried out for the present set of data. It must be admitted, however, that significant data are obtained only up to $q = 2\ \mathrm{nm}^{-1}$ owing to the influence of background scattering (fluorescence and scattering from water). Beyond this q value the noise of the scattering data makes a quantitative discussion difficult. Despite these problems the result displayed in Fig. 3 corroborates the model calculation in a qualitative fashion: The measured scattering intensity is lowered when approaching the absorption edge and the scattering curves are shifted in an almost parallel fashion. Moreover, the quotient of $I(q)$ obtained at two different energies, $I(q,E_1)/I(q,E_2)$, is found to be approximately constant as predicted by the present model for a high contrast of the macroion.

The latter point is corroborated by a comparison with theory that is displayed in Fig. 3. As in Ref. [16] a rather high electron density ($\Delta\rho_{\mathrm{rod}} = 25\mathrm{e/nm}^3$) must be assumed to match the data measured far away from the absorption edge. If a smaller value is used, neither the nonresonant intensity nor the resonant term can be described properly. This becomes obvious when calculating $I(q)$ for $\Delta\rho_{\mathrm{rod}} = 2\mathrm{e/nm}^3$. This leads to a much smaller cross-term and hence a much smaller effect of the anomalous dispersion on the measured data. Despite the rather large experimental error visible in Fig. 3 which is mainly due to the limited amount of sample material (about a factor of 10 apart from the optimal sample thickness) a much smaller difference between the two scattering curves can be ruled out. In this way ASAXS supplements the SAXS studies [16] in an important manner. Hence, all the SAXS and ASAXS data obtained on the rodlike polyelectrolyte under consideration here can be described by a single set of consistent parameters.

Conclusion

The analysis of stiff-chain polyelectrolytes by ASAXS has been considered. Model calculations based on the PB cell model demonstrated that an appreciable shift of the scattering curves should result if ASAXS measurements are conducted near the absorption edge of the counterions. The leading term of the correction (Eq. 15) is the cross-term of the normal scattering amplitude with the resonant part that only depends on the counterions. Hence, the contribution of the counterions to the measured scattering intensity can be discerned. The self-term (third expression in brackets of Eq. 15) is not negligible but is of opposite sign to the cross-term.

Preliminary experimental data suggest theory seems to underestimate the magnitude of resonant scattering but describes the experimental findings in an at least qualitative manner. It hence demonstrates that ASAXS is a useful tool to assess the correlation of the counterions with the linear macroion. In particular, ASAXS corroborates previous results obtained by SAXS. Further studies along the lines given here are under way.

Acknowledgement Financial support by the Deutsche Forschungsgemeinschaft, Schwerpunkt Polyelektrolyte, is gratefully acknowledged.

References

1. Katchalsky A (1971) Pure Appl Chem 26:327
2. Mandel M (1988) In: Mark FH, Bikales NM, Overberger CG, Menges G (eds) Encyclopedia of polymer science and engineering, vol 11, 2nd edn. Wiley, New York, p 739
3. Schmitz KS (1993) Macroions in solution and colloid suspension. VCH, New York
4. Förster S, Schmidt M (1995) Adv Polym Sci 120:51
5. Fuoss RM, Katchalsky A, Lifson S (1951) Proc Natl Acad Sci USA 37:579
6. Alfrey T, Berg PW, Morawetz H (1951) J Polym Sci 7:543
7. Le Bret M, Zimm B (1984) Biopolymers 23:287
8. Manning GS (1972) Ann Rev Phys Chem 23:117
9. Kassapidou K, Jesse W, Kuil ME, Lapp A, Egelhaaf S, van der Maarel JRC (1997) Macromolecules 30:2671
10. van der Maarel JRC, Kassapidou K (1998) Macromolecules 31:5734
11. van der Maarel JRC, Groot LCA, Mandel M, Jesse W, Jannink G, Rodriguez V (1992) J Phys II 2:109
12. Zakharova SS, Engelhaaf SU, Bhuiyan LB, Outhwaite CW, Bratko D, van der Maarel JRC (1999) J Chem Phys 111:10706
13. Huggins JS, Benoit HC (1994) Polymers and neutron scattering. Clarendon, Oxford
14. Wu CF, Chen SH, Shih LB, Lin JS (1988) Phys Rev Lett 61:645
15. Chang SL, Chen SH, Rill RL, Lin JS (1990) J Phys Chem 94:8025
16. Guilleaume B, Blaul J, Wittemann M, Rehahn M, Ballauff MJ (2000) Condens Matter 12:A245
17. Stuhrmann HB (1985) Adv Polym Sci 67:123
18. Stuhrmann HB, Goerigk G, Munk B (1991) In: Ebashi S, Koch M, Rubenstein E (eds) Handbook of synchrotron radiation, vol 4. Elsevier, Amsterdam, pp 555
19. Haubold HG, Gruenhagen K, Wagener M, Jungbluth H, Heer H, Pfeil A, Rongen H, Brandenburg G, Moeller R, Matzerath J, Hiller P, Halling H (1989) Rev Sci Instrum 60:1943
20. Haubold HG, Wang XH, Jungbluth H, Goerigk G, Schilling W (1996) J Mol Struct 383:283
21. Goerigk G, Haubold HG, Schilling W (1997) J Appl Crystallogr 30:1041
22. Goerigk G, Williamson DL (1998) Solid State Commun 108:419
23. Ding YS, Hubbard SR, Hodgson KO, Register RA, Cooper SL (1988) Macromolecules 21:1698
24. (a) Register RA, Cooper SL (1990) Macromolecules 23:310; (b) Register RA, Cooper SL (1990) Macromolecules 23:318
25. King GI, Mowery PC, Stoeckenius W, Crespi HL, Schoenborn BP (1980) Proc Natl Acad Sci USA 77:4726
26. Williams CE (1991) In: Lindner P, Zemb T (eds) Neutron, X-ray and light scattering. Elsevier, Amsterdam, p 101
27. Fournet G (1951) Bull Soc Fr Mineral Cristallogr 74:39
28. James RW (1948) The optical principles of the diffraction of X-rays. Bell, London
29. Cromer DT, Liberman DA (1981) Acta Crystallogr A 37:267
30. Marcus Y (1983) J Solution Chem 12:4